V. Interstellar Dust

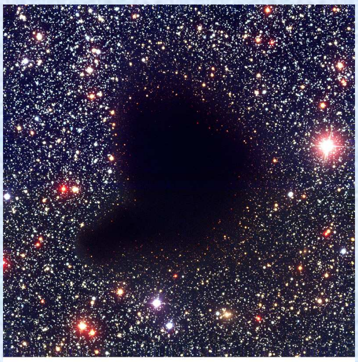

Dust becomes detectable as:

- Extinction (+ reddening in stellar spectra)
- Reflexion
- IR emission

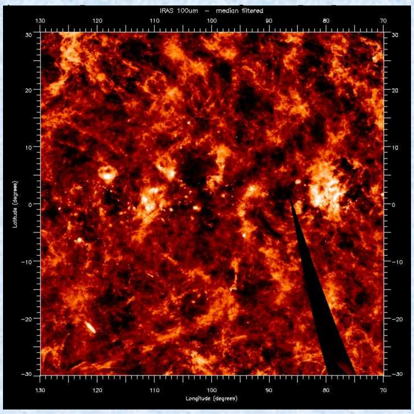

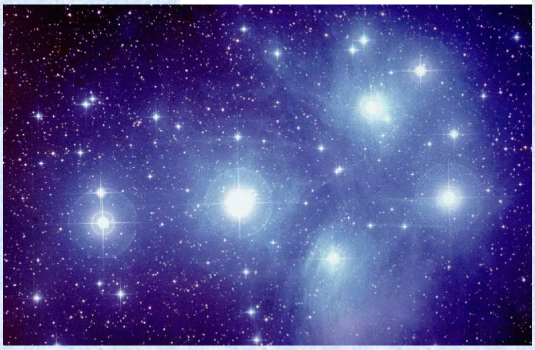

1. Interstellar Extinction and Reddening

R. J. Trumpler (1886-1956): studied a sample of open clusters and determined the distances to them in two ways:
- by measuring their angular diameter, and assuming that they all have the same physical size.
- from photometric distances (known sp. type and apparent magnitude).

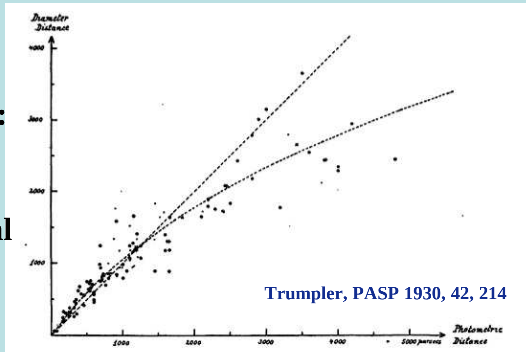

FIG. 1.—Comparison of the distances of 100 open star clusters determined from apparent magnitudes and spectral types (abscissae) with those determined from angular diameters (ordinates). The large dots refer to clusters with well-determined photometric distances, the small dots to clusters with less certain data (half weight). The asterisks and crosses represent group means. If no general space absorption were present, the clusters should fall along the dotted straight line; the dotted curve gives the relation between the two distance measures for a general absorption of $0^m.7$ per 1000 parsecs.

Photometric distances were systematically larger than the angular-diameter distances. Or, <u>magnitudes were systematically fainter</u> than those given by angular-diameter distances.

Dust Effects on Starlight:

1) Extinction (dimming of the light from stars)

- Scatters photons out of the line of sight from the star to the sun.
- Absorbs photons, converting their energy into heat (re-radiated in IR); the absorption is effective at wavelengths comparable to the size of the dust grains which have ~ 100 nm. So dust absorbs UV radiation most effectively.

For dust grains ~100 nm or larger: Mie scattering which has a weak dependence on wavelength (λ^{-1}); the smallest particles produce Rayleigh scattering, (λ^{-4}).

2) Reddening

- Broadband colors are affected because the extinction is higher at short wavelengths than at long wavelengths.

Note1: the interstellar dust does not affect (significantly) the spectra of stars; thus the spectral classification can be used to measure the amount of reddening and extinction.

Note2: the ISM is made of gas and dust; dust represents 1% of the ISM (by mass).

1.1. Interstellar Extinction

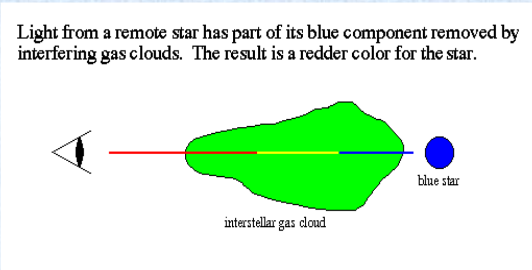

In the NIR dust-enshrouded stars become visible
⇒ dust particles have sizes of short optical wavelengths

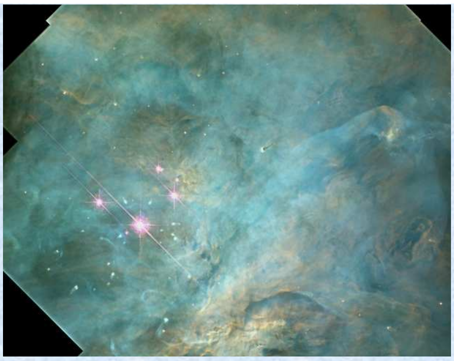

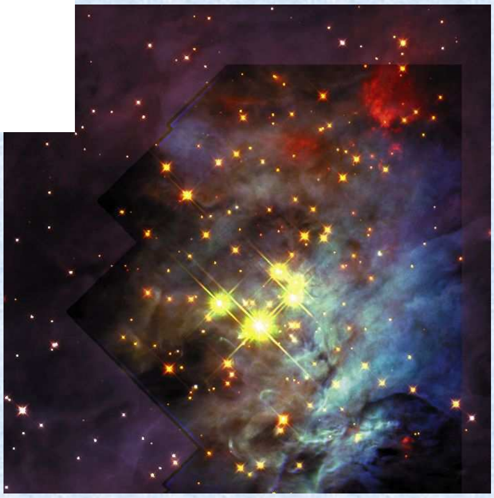

1.2. Reddening

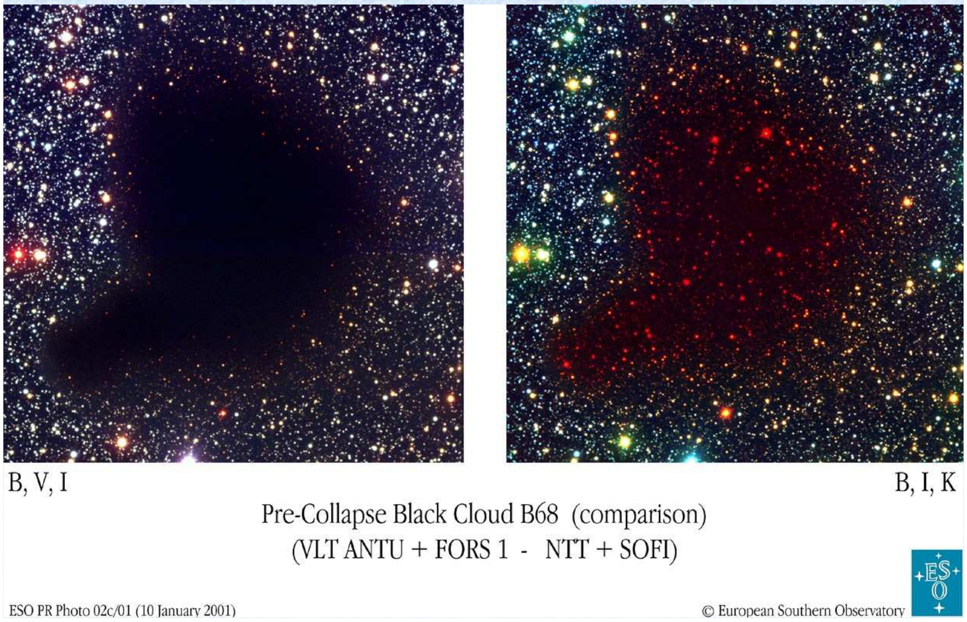

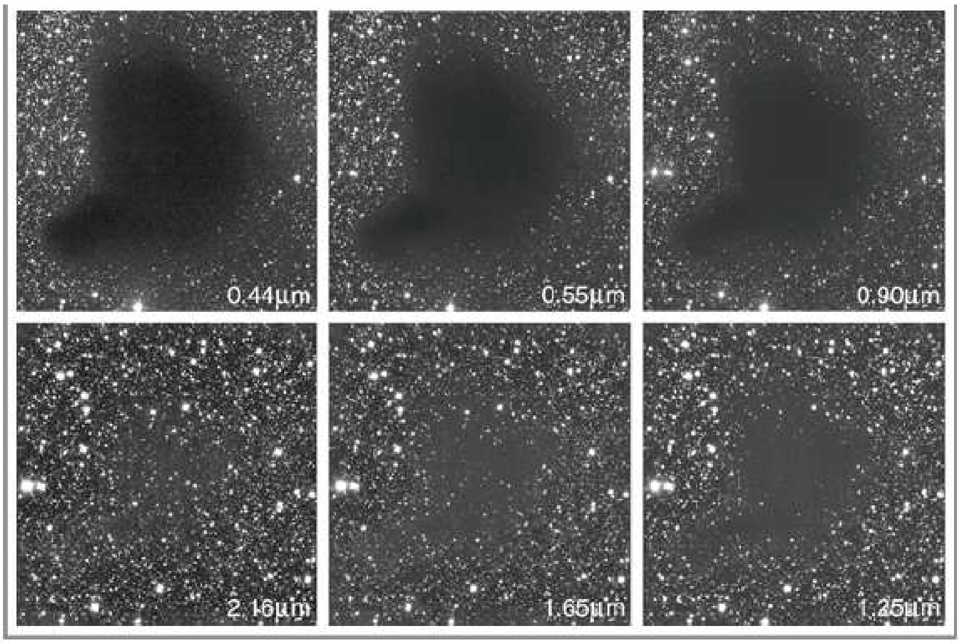

<u>Measuring the Reddening E(B-V)</u>

1) From stars

a) individual stars, b) star clusters

If the intrinsic color of a star is known from the spectral type, then this can be compared to the measured color, and therefore the reddening determined. The best stars for this job are O and B types because:

1) they are highly luminous and can thus be seen at large distances over which reddening can accumulate to large values

2) they are intrinsically blue and thus susceptible to reddening

3) they have distinctive spectra that can be classified with high precision

From measurements of O,B stars it was found that in the two-color diagram, reddening moves stars along a line with a measurable slope. This line, aka the <u>reddening vector</u>, has a slope:

$$E(U-B)/E(B-V) = 0.72.$$

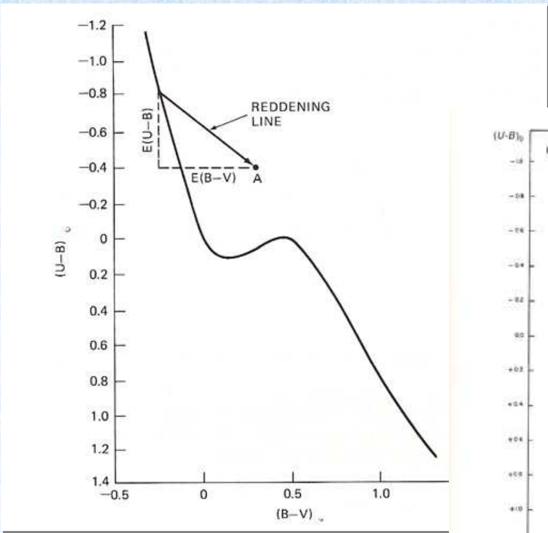

Henden & Kitchuck

Smith

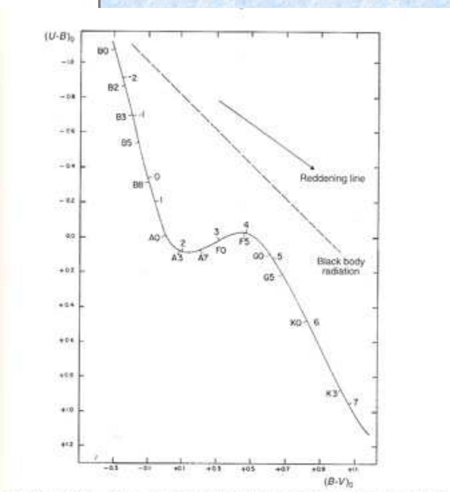

Fig. 8.4. The $(U-B, B-V)$ two-colour diagram for main-sequence stars. Note that $U-B$ is conventionally plotted as increasing downwards. The theoretical relationship for black bodies is also shown. The reddening line is explained in Section 12.2. (©1963 by The University of Chicago. All rights reserved.)

Reddening-free indices

Based on the slope E(U-B)/E(B-V), it is possible to define a parameter that depends only on the spectral type of the star and it is independent of the reddening. This parameter is:

$Q = (U\text{-}B) - E(U\text{-}B)/E(B\text{-}V)\ (B\text{-}V) = (U\text{-}B) - 0.72\ (B\text{-}V) = (U\text{-}B)_0 - 0.72\ (B\text{-}V)_0$

For stars with known MK spectral types, Q is calculated, to obtain a calibrating curve. Then, for stars with unknown spectral types (faint stars, distant stars), just by measuring their UBV, (i.e. Q), we can determine the spectral type, and intrinsic colors $(B\text{-}V)_0$ for instance. Once the intrinsic color index is known, the reddening E(B-V) can be determined. Thus, it can be shown:

$(B\text{-}V)_0 = 0.332\ Q$ and $E(B\text{-}V) = (B\text{-}V) - 0.332\ Q$

This method is applicable only for *spectral types earlier than A0* (because of the shape of the two color curve; Q is no longer a unique function of sp. type).

Reddening-free indices can be defined in other photometric systems (e.g. Stromgren).

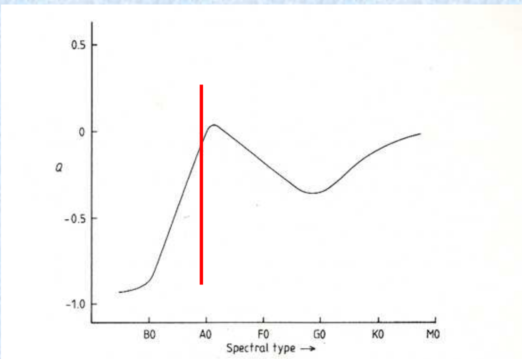

Figure 3.1.17 Variation of colour factor with spectral type.

Q as a function of spectral type and $(B\text{-}V)_0$. The limit for the use of Q is A0 or $(B\text{-}V)_0 = 0$.

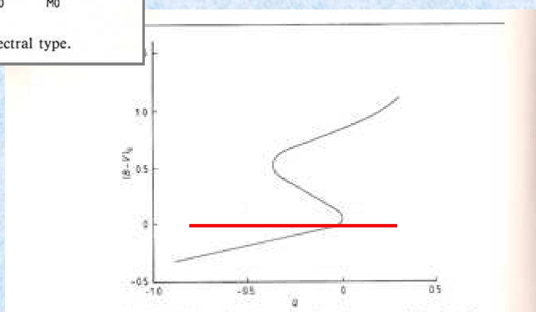

Figure 3.1.18 Relationship between colour factor and the $B-V$ intrinsic colour index.

Kitchin

Determining the reddening in the field of a star cluster

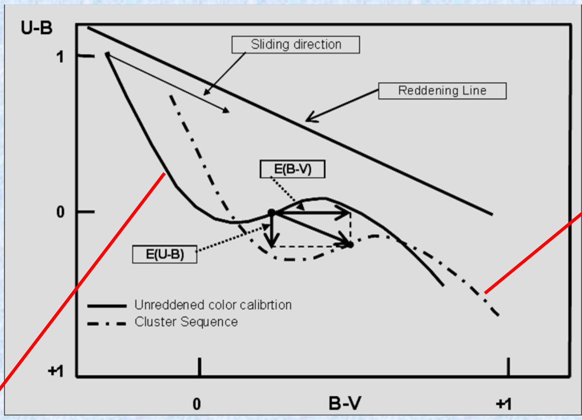

Cluster sequence (observations)

Fiducial line (theoretical models)

1.3. Definitions:

Extinction: $A_\lambda = m_\lambda - m_{\lambda,0}$

Colour Excess: $E_{\lambda_1 - \lambda_2} = (m_{\lambda_1} - m_{\lambda_2}) - (m_{\lambda_1} - m_{\lambda_2})_0$

$= (m_{\lambda_1} - m_{\lambda_{1.0}}) - (m_{\lambda_2} - m_{\lambda_{2.0}})$

$= A_{\lambda_1} - A_{\lambda_2}$

in particular: $E_{B-V} = (B - V) - (B - V)_0$

$= (B - B_0) - (V - V_0)$

$= A_B - A_V$

Determination of discoloration $A_{\lambda_1} - A_{\lambda_2}$ with help of 2 stars of same SpT and Lum.Class but different distances to different directions are only to a constant factor of the **mass absorption coefficient** k_λ possible. Thus,

normalized extinction: $\boxed{\frac{E_{\lambda-V}}{E_{B-V}} = \frac{A_\lambda - A_V}{A_B - A_V} = F_\lambda} = \frac{\Delta m_\lambda - \Delta m_V}{\Delta m_B - \Delta m_V} = \frac{k_\lambda - k_V}{k_B - k_V}$

2. Extinction Curve

Normalized extinction larger at smaller wavelengths:

$F_\lambda \sim \lambda^{-1}$

$\Rightarrow$ **Reddening** of passing light;

For $\lambda \to \infty$ $F_{\lambda \to \infty} \to -3$

$\Rightarrow$ **$A_V / E_{B-V} = R_V \sim 3.1$**

bump at 2200 Å

knee at 4400 Å

Savage & Mathis (1979) ARAA 17

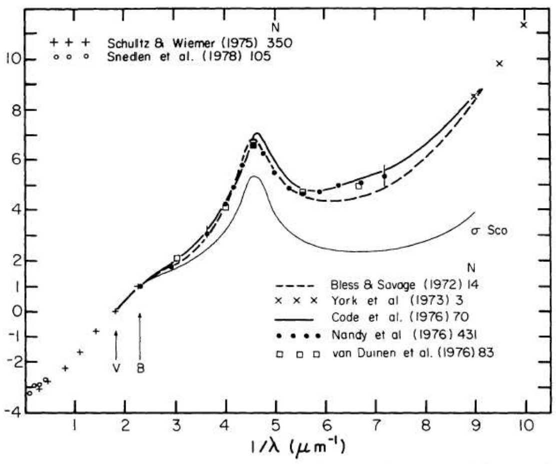

Figure 1 Average normalized interstellar extinction is plotted versus $1/\lambda$ in μm^{-1}. $E(\lambda-V)$ refers to the extinction in magnitudes between a wavelength λ and the photoelectric V band. The references for the various curves are provided along with an indication of how many stars were used to derive each average curve. One abnormal ultraviolet curve for σ Sco from Bless & Savage (1972) is also shown. The average curves plotted can be converted to total normalized extinction, $A_\lambda/E(B-V)$, by adding $R = 3.1$ to the quantity plotted. Note that the normalization to $E(B-V) = 1$ implies a corresponding hydrogen column density of $N(HI + H_2) = 5.8 \times 10^{21}$ atoms cm^{-2} (see Section 2). The error bars on two of the TD-1 points (Nandy et al. 1976) give an indication of the maximum observed variation in the *average* extinction curves derived for different galactic regions.

Table 2 An average interstellar extinction curve

	$\lambda(\mu m)$	$\lambda^{-1}(\mu m^{-1})$	$E(\lambda-V)/E(B-V)$	$A_\lambda/E(B-V)$
	∞	0	−3.10	0.00
L	3.4	0.29	−2.94	0.16
K	2.2	0.45	−2.72	0.38
J	1.25	0.80	−2.23	0.87
I	0.90	1.11	−1.60	1.50
R	0.70	1.43	−0.78	2.32
V	0.55	1.82	0	3.10
B	0.44	2.27	1.00	4.10
	0.40	2.50	1.30	4.40
U	0.344	2.91	1.80	4.90
	0.274	3.65	3.10	6.20
	0.250	4.00	4.19	7.29
	0.240	4.17	4.90	8.00
	0.230	4.35	5.77	8.87
	0.219	4.57	6.57	9.67
	0.210	4.76	6.23	9.33
	0.200	5.00	5.52	8.62
	0.190	5.26	4.90	8.00
	0.180	5.56	4.65	7.75
	0.170	5.88	4.77	7.87
	0.160	6.25	5.02	8.12
	0.149	6.71	5.05	8.15
	0.139	7.18	5.39	8.49
	0.125	8.00	6.55	9.65
	0.118	8.50	7.45	10.55
	0.111	9.00	8.45	11.55
	0.105	9.50	9.80	12.90
	0.100	10.00	11.30	14.40

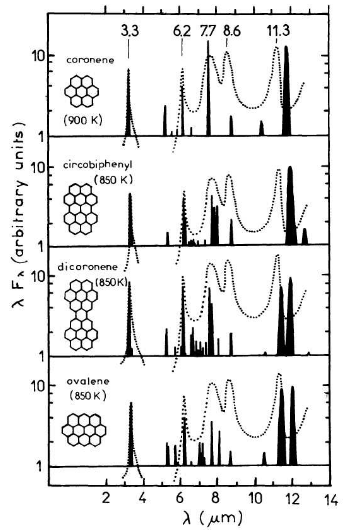

Figure 5 Emission spectra of several compact PAHs calculated from their laboratory-measured absorption spectra (in solid phase) using Equation 3 (from Léger et al. 1988b). The spectrum of the reflection nebula NGC 2023 is reported for comparison (dotted line). It is deduced from observations by Sellgren et al. (1985) except for the 6.2-μm band, which was not resolved and whose shape is assumed to be similar to that of M82 (Willner et al. 1977). The only free parameter in the calculation is the emission temperature, which is adjusted to reproduce the observed ratio of the CH bands at 3.3 and 11.3 μm (adopted T_c is in parentheses). Note the accurate agreement of bands at 3.3 and 6.2 μm between the observations and the compact PAH spectra. The poor wavelength match at 11–14 μm is discussed in Section 2.6.

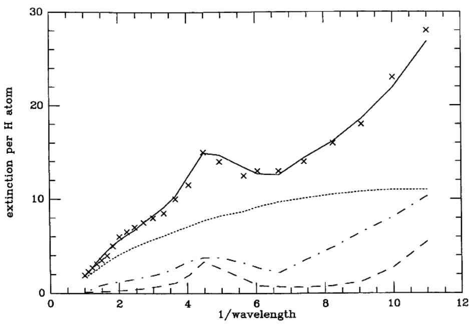

Figure 9 Measured average extinction curve (crosses), expressed as σ_H, as a function of the inverse wavelength (in microns). The dotted line shows the standard grain contribution, the dashed line the carbonaceous VSG contribution, and the dot-dash line the PAH contribution. The sum is shown as the solid line. The unit for the cross section in 10^{-22} cm^{-2}.

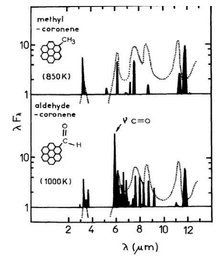

Figure 6 Emission spectra of PAHs with attached radical. The presence of methyl groups in the interstellar mixture appears possible, but that of abundant aldehyde groups is excluded.

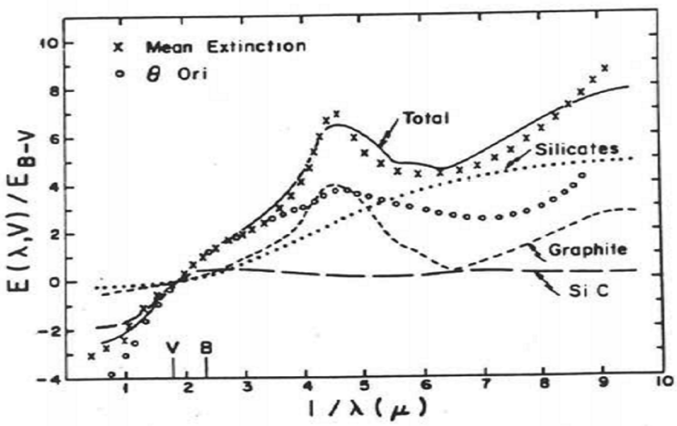

Figure 7.2 Dependence of selective extinction on wavelength. The ratio of $E(\lambda, V)$ to E_{B-V} is plotted against the reciprocal wavelength in microns. The crosses give the mean observed extinction for normal stars [2]; in the ultraviolet these are based on 14 observed stars, excluding 3 abnormal ones; the circles give observed values for $\theta^1 + \theta^2$ Ori, showing abnormal extinction. The other curves are computed theoretically [16] for grains of three different types (see text), with the sum of the three shown by the solid line.

The Extinction Curve (cont.)

UV peak at ~ 220 nm

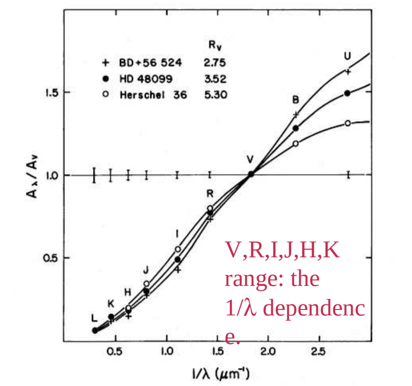

FIG. 3.—Comparison between the mean optical/NIR R_V-dependent extinction law from eqs. (2) and (3) and three lines of sight with largely separated R_V values. The wavelength position of the various broad-band filters from which the data were obtained are labeled (see Table 3). The "error" bars represent the computed standard deviation of the data about the best fit of $A(\lambda)/A(V)$ vs. R_V^{-1} with $a(x) + b(x)/R_V$ where $x \equiv \lambda^{-1}$. The effect of varying R_V on the shape of the extinction curves is quite apparent, particularly at the shorter wavelengths.

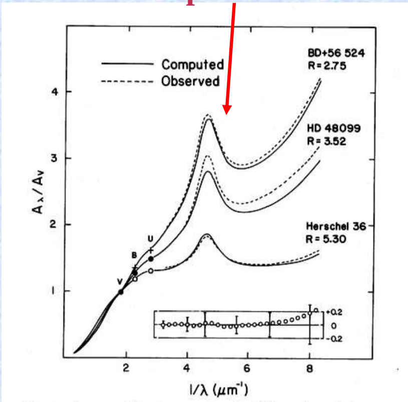

FIG. 4.—Same as Fig. 3 except for the UV portion of the mean R_V-dependent extinction law from eq. (4). The data at U, B, and V from Fig. 3 are also plotted. Again, the "error" bars in the lower inset represent the computed standard deviation of the data about the best fit of $A(\lambda)/A(V)$ vs. R_V^{-1} with $a(x) + b(x)/R_V$. The open symbols in the inset represent the difference between $A(\lambda)/A(V)$ from eq. (4) and the average curve of Seaton (1979) for $R_V = 3.2$. The only serious deviation occurs for $x > 7\ \mu m^{-1}$ (see text).

In the V band and at shorter wavelengths the curve varies with los, i.e., the slope (or R_V) changes: different sizes of dust grains (see also, fig 3.17 in BM).

Cardelli, Clayton, Mathis 1989

Extinction curve (fig 3.17 BM - on a log scale; from Mathis 1990)

Far UV

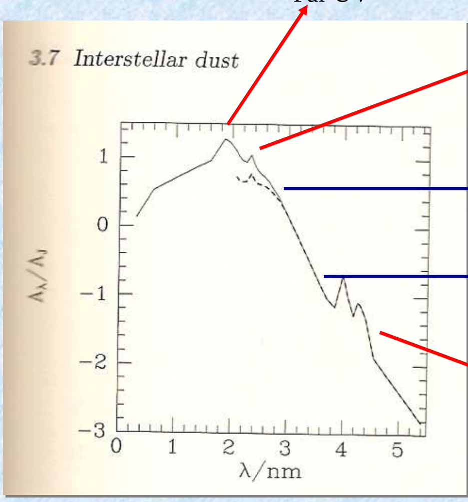

UV peak at ~ 220 nm

(tiny graphite pieces ~ 50 atoms!)

The V,R,I,J,H,K range; the 1/λ dependence.

2 peaks in IR (9.7 and 18 μm)

(origin? Silicate grains…)

The 2 curves (cont. and dashed correspond to two lines of sight).

Measuring the Reddening E(B-V): HI and IR emission

But, the ISM is clumpy and the column density varies with l.o.s. Therefore maps of E(B-V) have been determined from

1) H I distribution (and column density) + galaxy counts - Burstein & Heiles (1982) for |b| > 10 deg. (outside of the zone of avoidance); the 21 cm emission line of H I AND the distribution of galaxies (assumes they have a uniform distribution; no clusters).
2) IR emission (COBE and IRAS) + maps of H I emission; Schlegel et al. (1998) (www.astro.princeton.edu/~schlegel/dust); has a resolution of 6.1 arcmin; it is meant to supersede the BH (1982) maps in accuracy and spatial resolution.

-found to overestimate visual extinction by a factor of 1.16 (Chen et al. 1999), or more in region with high extinction (Arce & Goodman 1999, Amores & Lepine 2007),

1) Extinction A_V

In a given waveband (for example V band):

$A_V = m_V - m_{V,0}$

m_V - apparent V-band magnitude

$m_{V,0}$ - apparent magnitude in the absence of dust

And:

$m_V = M_V + A_V + 5 \log d - 5$

$m_{V,0} = M_V + 5 \log d - 5$ ---> $m_{V,0} - M_V = 5 \log d - 5$ aka the distance modulus

If the MK type of the star is known, as well as the distance, A_V can be determined. In practice, d is not known.

2) Reddening (or color excess) - E(B-V)

For a given color:

$E(B\text{-}V) = A_B - A_V = (B\text{-}V) - (B\text{-}V)_0$

E(B-V) - reddening

A_B, A_V - extinction in B and V bands

(B-V) - reddened color

$(B\text{-}V)_0$ - dereddened color (or unreddened color, or intrinsic color).

3) The ratio of extinction to reddening (or total to selective absorption): R_V

$$R_V = \frac{A_V}{A_B - A_V} = \frac{A_V}{E(B-V)}$$

This ratio is usually known to be approximately constant with the line of sight (~ 3). Adopting this R_V and a known E(B-V), the absorption can be determined.

The reddening E(B-V) can be determined:

a) By comparing observed colors with colors derived from the spectral type

b) From multicolor photometry

c) From reddening maps derived for the entire Galaxy (not very accurate)

What Determines the Amount of Extinction and Reddening?

1) Extinction and reddening depend on wavelength. This dependence is known as the extinction curve.

2) The amount of extinction and reddening *along a line of sight* depends on

a) the amount of dust along it (that is, the distance to a star)

b) the dust properties - e.g., size of dust grains.

If the *type of dust* were everywhere the same, the extinction curve would be everywhere the same. This appears to be the case in most regions in our Galaxy; there are however regions where the extinction curve changes from the standard one (e.g., within molecular clouds).

The Extinction Curve:

represents the variation of the extinction A (mags) as a function of wavelength λ

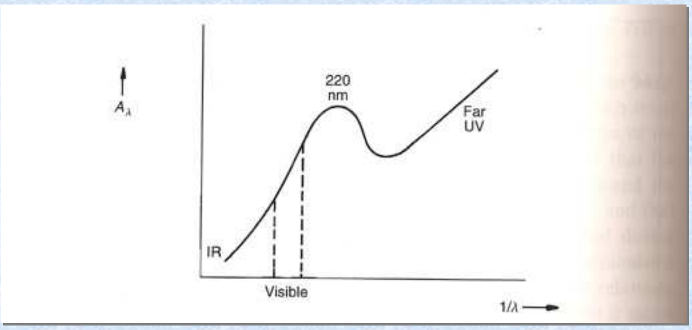

Smith

-In V and redward of V the dependence is nearly linear (~ $1/\lambda$)

-Blueward of V, the extinction varies, with a peak in the UV at 220 nm.

-In the far UV, extinction decreases more steeply with λ than $1/\lambda$.

The Extinction Curve (cont.)

Other representations of the extinction curve:

- $A_\lambda/A_J = f(\lambda)$
- $A_\lambda/ E(B\text{-}V) = f(\lambda)$
- $E(\lambda - V)/E(B\text{-}V) = f(\lambda)$.

-Cardelli, Clayton and Mathis (1989) have shown that:

$$\frac{A_\lambda}{A_J} = a(\lambda) + \frac{b(\lambda)}{R_V}$$

a,b - are polynomials

- It can be shown that the slope of the extinction curve near V is $A_V/(A_J R_V)$; where $R_V = A_V/E(B\text{-}V)$. Thus R_V quantifies whether the curve is rising steeply into UV or not: 3 is for a steeply rising curve, 5 is for a slowly rising curve. Classical studies of extinction give R_V = 3.1 - 3.2.

The extinction curve expressed per waveband

Table 3.21 The standard interstellar extinction law

Band X	$\frac{E(X-V)}{E(B-V)}$	$\frac{A_X}{A_V}$
U	1.64	1.531
B	1.00	1.324
V	0.00	1.000
R	−0.78	0.748
I	−1.60	0.482
J	−2.22	0.282
H	−2.55	0.175
K	−2.74	0.112
L	−2.91	0.058
M	−3.02	0.023
N	−2.93	0.052

SOURCE: From data published in Rieke & Lebofsky (1985)

Binney & Merrifield

David Schlegel, Durham, 26 Jan 1998

Extinction in Different Bandpasses

Assuming an R_V=3.1 extinction curve, the dust maps should be multiplied by the value in the final column to determine the extinction in a given passband. The standard optical-IR bandpasses are represented by the CTIO and UKIRT transmission curves. For further details, see Appendix B of the text.

Filter name	LamEff	A/A(V)	A/E(B-V)
Landolt U	3372	1.664	5.434
Landolt B	4404	1.321	4.315
Landolt V	5428	1.015	3.315
Landolt R	6509	0.819	2.673
Landolt I	8090	0.594	1.940
CTIO U	3683	1.521	4.968
CTIO B	4393	1.324	4.325
CTIO V	5519	0.992	3.240
CTIO R	6602	0.807	2.634
CTIO I	8046	0.601	1.962
UKIRT J	12660	0.276	0.902
UKIRT H	16732	0.176	0.576
UKIRT K	22152	0.112	0.367
UKIRT L'	38079	0.047	0.153
Gunn g	5244	1.065	3.476
Gunn r	6707	0.793	2.590
Gunn i	7985	0.610	1.991
Gunn z	9055	0.472	1.540
Spinrad R	6993	0.755	2.467
APM b_J	4690	1.236	4.035
Stromgren u	3502	1.602	5.231
Stromgren b	4676	1.240	4.049
Stromgren v	4127	1.394	4.552
Stromgren beta	4861	1.182	3.858
Stromgren y	5479	1.004	3.277
Sloan u'	3546	1.579	5.155
Sloan g'	4925	1.161	3.793
Sloan r'	6335	0.843	2.751
Sloan i'	7799	0.639	2.086
Sloan z'	9294	0.453	1.479
WFPC2 F300W	3047	1.791	5.849
WFPC2 F450W	4711	1.229	4.015
WFPC2 F555W	5498	0.996	3.252
WFPC2 F606W	6042	0.885	2.889
WFPC2 F702W	7068	0.746	2.435
WFPC2 F814W	8066	0.597	1.948
DSS-II g	4814	1.197	3.907
DSS-II r	6571	0.811	2.649
DSS-II i	8183	0.580	1.893

Schlegel 1998: to be used in home works, etc.

Measurements of R_V in various lines of sight to O, B stars

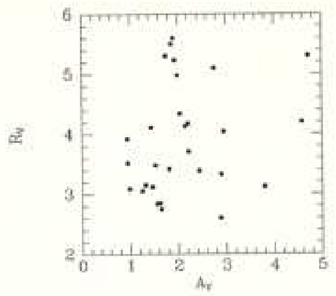

Figure 3.18 Values of R_V for 28 lines of sight to O and B stars [From data published in Cardelli, Clayton & Mathis (1989)]

Binney & Merrifield

3. Interstellar Extinction

Extinction by dark clouds reduce stellar brightness m_V by A_V

$\Rightarrow$ **distance module** must be corrected by $\mathbf{A_V}$:

$$m_V - M_V = 5 \log d - 5 + A_V$$

$< A_V > \approx 1^m \, \mathrm{kpc}^{-1}$

$\mathbf{E_{B-V}}$ correlates better with column dens. of molecular gas than of pure atomic gas

$\Rightarrow$ dust is combined with mol.clouds

50% of the IS metals are bound in dust!

Savage & Mathis (1979) ARAA 17

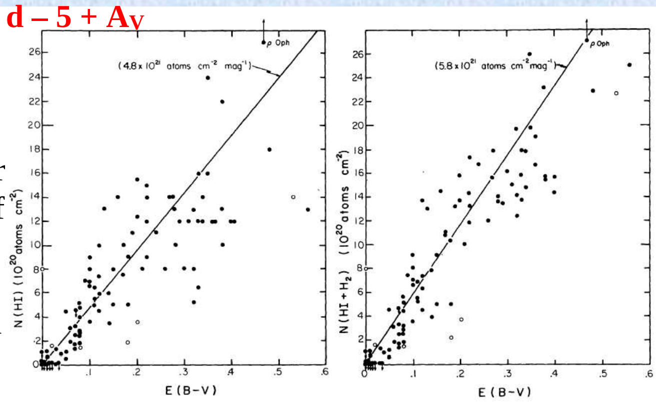

Figure 2 Correlations between gas column densities and interstellar reddening for 100 stars from the *Copernicus* atomic and molecular hydrogen survey (Savage et al. 1977, Bohlin, Savage & Drake 1978): (*a*) shows the atomic hydrogen column density, N(HI), versus $E(B-V)$, (*b*) shows the total hydrogen column density, $N(HI+H_2) = N(HI)+2N(H_2)$, versus $E(B-V)$. Be stars are denoted with the open symbols. The solid line in (*a*) gives the average *atomic* hydrogen to $E(B-V)$ ratio 4.8×10^{21} atoms cm^{-2} mag^{-1}. In (*b*) the solid line gives the average *total* hydrogen to $E(B-V)$ ratio of 5.8×10^{21} atoms cm^{-2} mag^{-1}. The point for ρ Oph in (*a*) and (*b*) should be moved upward by about a factor of 2.7.

Measuring the Reddening E(B-V)

2) From HI and IR emission

It was found that approximately along any l.o.s. E(B-V) is *proportional* to the column density N_H of interstellar hydrogen atoms, irrespective of whether the hydrogen atoms are in atomic H I, or molecular form H_2 (Bohlin et al. 1978, Fig. 8.14 BM). Specifically,

$$E(B-V) = \frac{N_H}{5.8\times10^{25}\,m^{-2}}$$

The density of H near the Sun is $n_H=10^6\ m^{-3}$. To first approximation in the solar neighborhood, the column density can be expressed:

$$N_H(m^{-2}) \cong 3.1\times10^{25}\,d(kpc)$$

And,

$$E(B-V) \cong 0.53d(kpc)$$

$$A_V \cong 1.6d(kpc)$$

Other approximations: A_V = 0.7 - 1.0 mag/kpc

4. Dark Clouds

examples: Coalsack
BHR 71
Barnard68 ($A_V \approx 20^m$)
Horsehead Nebula

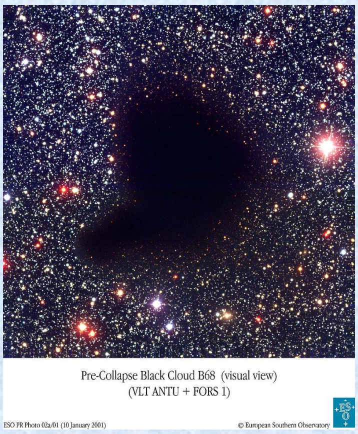

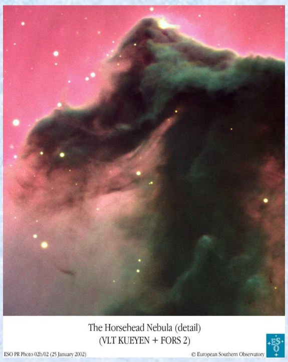

Cloud location determined by **Wolf diagrams**

Neckel & Klare 1960

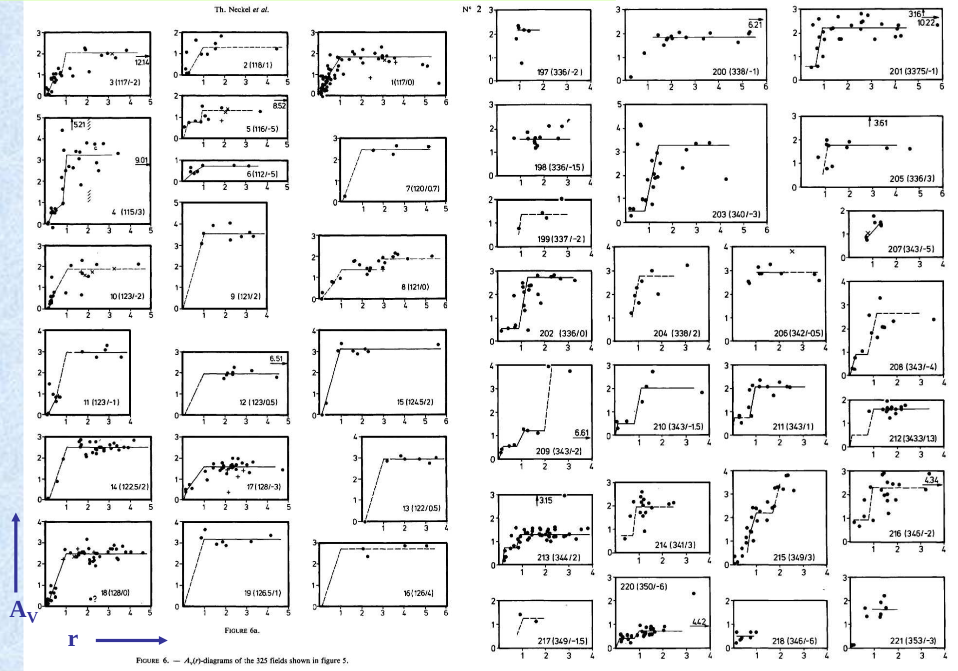

FIGURE 6. — $A_v(r)$-diagrams of the 325 fields shown in figure 5.

5. Galactic Distribution

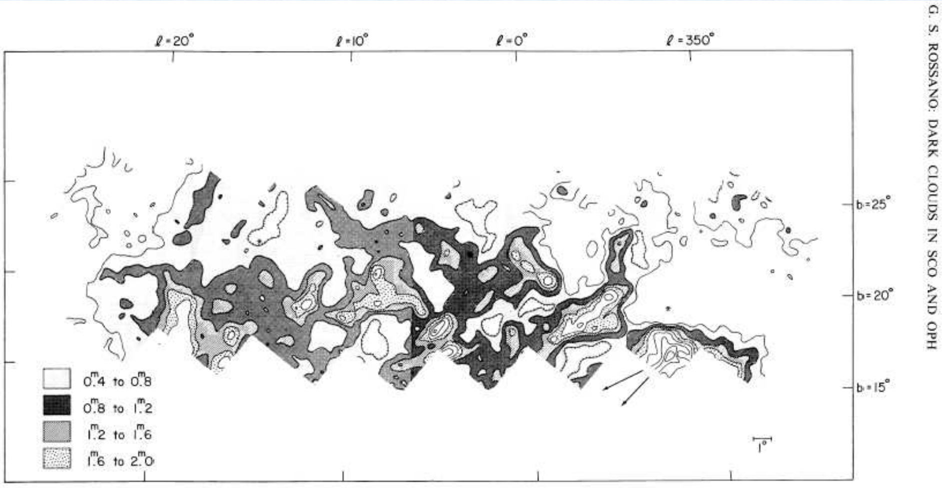

FIG. 1. The distribution of extinction in Scorpio and Ophichus. Contours are shown for extinctions of 0.4, 0.8, 1.2, 1.6, 2.0, 2.5, 3.0, 3.5, and 4.0 mag. To avoid ambiguity, the first four contour levels are shaded (light dots, heavy dots, parallel lines, equal signs).

INTERSTELLAR EXTINCTION

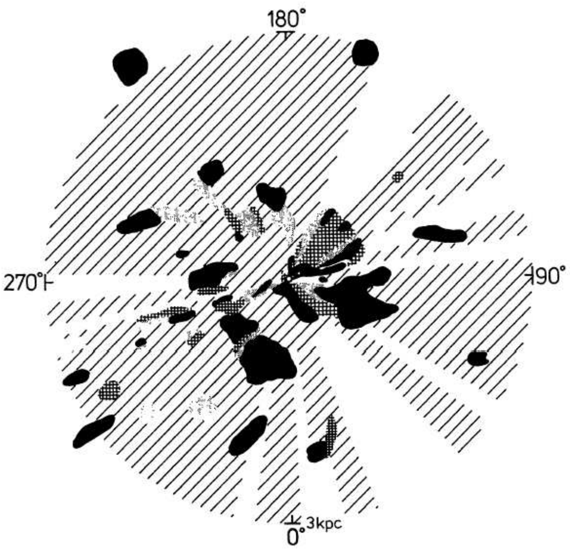

FIGURE 9a. — The galactic distribution of the dust for $r \leq 3$ kpc
$a_v = A_v/\text{kpc} < 1^m0/\text{kpc}$
$1^m0/\text{kpc} \leq a_v < 2^m0/\text{kpc}$
$2^m0/\text{kpc} \leq a_v < 3^m0/\text{kpc}$
$a_v \geq 3^m0/\text{kpc}$

Applying Wolf's diagrams one can derive the distribution of dust concentrations in the solar vicinity (see Part II).

Neckel & Klare 1980

IRAS - 100 µm

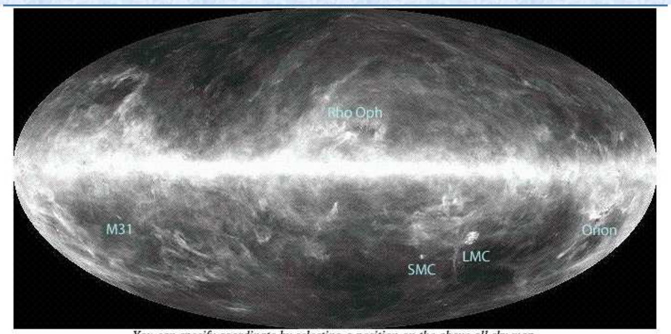

You can specify coordinate by selecting a position on the above all sky map.

Computes the interstellar reddening for a line of sight and/or region of the sky, returning the corresponding 100 um intensity, reddening maps, region statistics and estimated Galactic extinction. The reddening is derived using the data and technique that Schlegel, Finkbeiner & Davis (1998) pioneered combining the strengths of IRAS and COBE/DIRBE. The user should beware that the technique is restricted by both spatial resolution limitations and assumptions that are used to derive the dust temperature along the line of sight. Read more on the science background, technique and cautionary notes here . The image above shows an All Sky view of the IRAS 100 um imaging data, representing a MONTAGE-generated combination of the individual images created by Schlegel, Finkbeiner & Davis (1998).

irsa.ipac.caltech.edu/applications/DUST

SFD (1998) - IRAS + COBE

Models of the Extinction as a Function of Distance from the Sun

The reddening maps give the reddening at "infinity", i.e., all the reddening along the line of sight; this is ok for distant objects such as globular clusters. However, for more nearby stars, reddening models are used.

$$\frac{E(B-V)(r,l,b)}{E(B-V)(\infty,l,b)}$$

$$= 1 - \exp\left(-\frac{r\sin b}{h_{\rm red}}\right) \quad \text{if} \quad b \geq 0^\circ$$

$$\frac{1-\exp(-\frac{r\sin b}{h_{\rm red}})}{1-2\exp\left(\frac{Z_{\rm Sun}}{h_{\rm red}}\right)} \quad \text{if} \quad b < 0^\circ \quad \text{and} \quad r|\sin b| \leq Z_{\rm Sun}$$

$$\frac{1-2\exp\left(\frac{Z_{\rm Sun}}{h_{\rm red}}\right)+\exp\left(\frac{2Z_{\rm Sun}+r\sin b}{h_{\rm red}}\right)}{1-2\exp\left(\frac{Z_{\rm Sun}}{h_{\rm red}}\right)}$$

$$\text{if} \quad b < 0^\circ \quad \& \quad r|\sin b| > Z_{\rm Sun} \qquad (4)$$

$E(B-V)(\infty,l,b)$ is the reddening at "$r = \infty$", which is obtained directly from SFD map. These equations were derived by assuming the Sun is above the galactic plane, but similar equations can be obtained if the Sun is below it.

r - distance from the Sun to the target object

h_{red} = 100 pc (scale height of the absorbing material; from HI)

Z_{sun} ~ 20 pc

Chen et al. 1999 A&A, 352, 459

6. Dust Particles

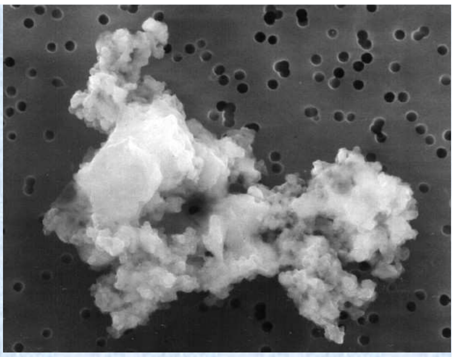

Dust can be in situ studied within our Solar System;

almost identical with IS dust: irregular fractal structure, grain sizes different depending on location and composition:

- **Silicates,**
- **Graphite,**
- **SiC, and**
- **PAHs (polycyclic aromatic Hydrogenes)**

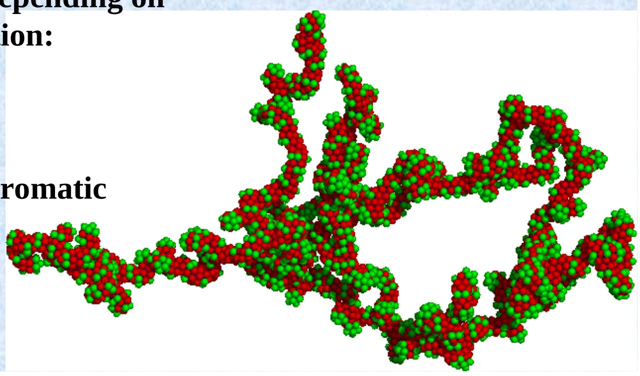

6.1. Dust Formation

Like molecules, dust is formed in dense cool metal-rich regions

cool:	red giant atmospheres and winds MC cores
dense: (+metal-rich)	interstellar shocks shock fronts of Supernovae Wolf-Rayet winds

WR 104

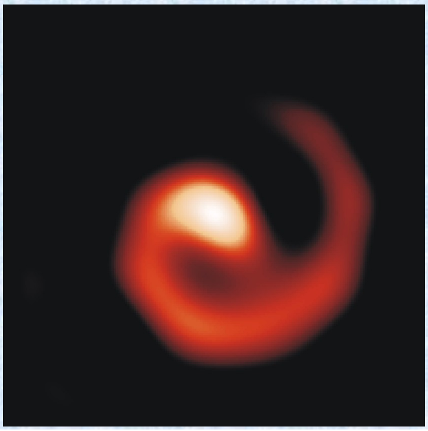

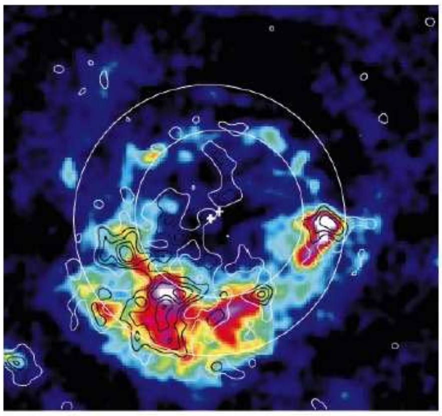

Figure 4 The 850 μm emission once the synchrotron has been subtracted using an 83-GHz image[19]. The box is 8.4 arcmin by 7.8 arcmin, north is up and east is left. Colours represent the 850 μm intensity, contours are the 450 μm emission with the synchrotron subtracted, starting at 3σ with increments of $+1\sigma$. The rings and crosses indicate the location (and centroids) of the forward and reverse shocks as determined from Chandra X-ray data[18]. The forward shock is at a mean radius of $153 \pm 12''$ and the reverse shock is at a mean radius of $95 \pm 10''$. The bulk of the dust emission appears to be bounded by the shocks, where the gas density is highest. There is a noticeable asymmetry in the dust emission.

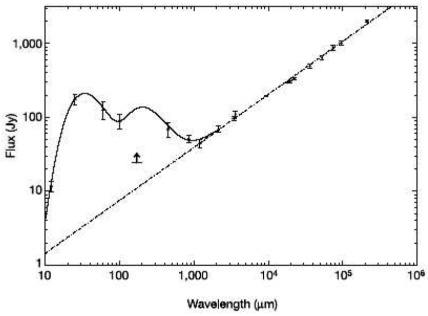

Figure 2 The SED of Cas A from the mid-infrared to the radio. All fluxes are integrated. The radio spectrum is fitted with a power-law slope with spectral index $\alpha = -0.72$. The radio data[19,23–28] have been scaled to the epoch of our Cas A observation (1998.4) using a recent study[23] which found that the flux decrease of Cas A was independent of frequency at about 0.6–0.7% yr^{-1}. The IRAS points are the averages of the literature values[13,29] with the error bars indicating the range of fluxes. SCUBA fluxes are 50.8 ± 5.6 Jy at 850 μm and 69.8 ± 16.1 Jy at 450 μm. The synchrotron contribution is 34.9 Jy at 850 μm and 22.1 Jy at 450 μm. The fit to the far-infrared/submm points is for a two-temperature grey body with $\beta = 0.9$, $T_w = 112$ K, $T_c = 18$ K and for 700 times more mass in the cold component than in the hot. We have fitted five parameters to six data points and therefore the fit is just constrained. The uncertainties in the SED parameters are given in Table 1. Clearly, the submm points at 450 and 850 μm lie above the extrapolation of the radio synchrotron spectrum. The point at 1.2 mm (ref. 28) is not of sufficient accuracy to determine an excess, but is consistent with our higher frequency measurements. Longer wavelength ISO measurements[30] of Cas A at 170 μm suggested that dust at ~30 K may have been present (implying of order $0.15 M_\odot$ of dust), however, the poor angular resolution of ISO at these wavelengths made a separation of the remnant and background emission impossible. The ISO flux is therefore a lower limit (R.J. Tuffs, personal communication).

6.2. Dust Destruction

Sputtering

Collisions with gas atoms, photons and other dust grains causes interstellar dust to breakdown and dissolve. This is called sputtering.

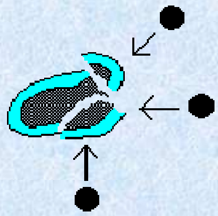

Because of sputtering, dust grains only survive in the cores of cold, dense molecular clouds.

7. Reflexion Nebulae

Reflection nebula are caused by the forward scattering of light from a nearby hot star by a dust cloud.

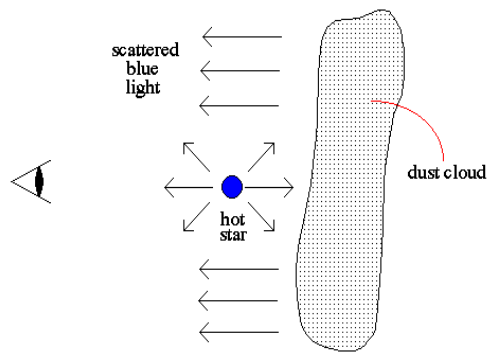

Complementary to extinction the reflected starlight is bluished because the scattering is larger at small λ.

8. Infrared Emission

Interstellar dust forms in the envelopes around red supergiants. Their structure is a carbon/silicate core often surrounded by water or carbon dioxide ice. Collisions with atoms causes the dust to emit a thermal spectrum in the IR.

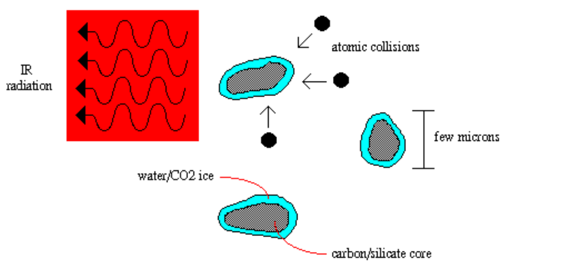

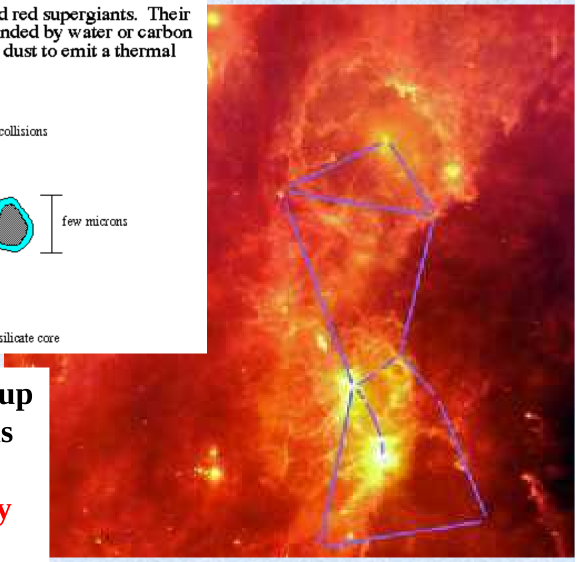

Stellar radiation also heats up the dust. Absorbed energy is thermalized.
Dust emission as black-body radiation according to the dust temperatur.

5.7. Dust temperature

344 HEILES

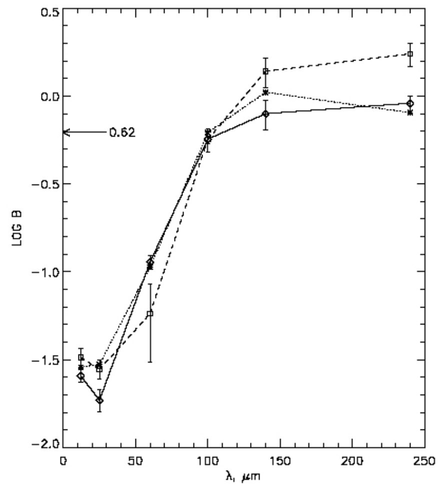

FIG. 5.—B is the logarithm of the IR brightness (MJy sr^{-1}) per 10^{20} H nuclei in the neutral gas; the arrow marks the global average. Dashed and solid lines are for the top and bottom regions in Fig. 4, respectively; the dotted line and global average are from Arendt et al. (1998).

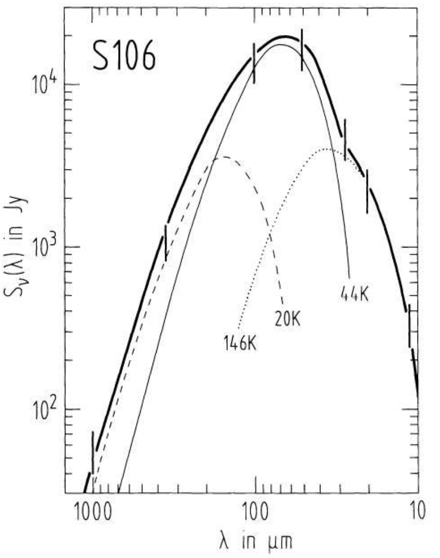

Fig. 3. Dust emission spectrum of S 106 between λ 10–1300 μm integrated over an area of $\sim$2$'$.5 × 2$'$.5. We adopted uncertainties of ±30% for all flux densities, except for the λ 350 μm integrated flux density, which we consider to be a lower limit (see text). The spectrum is decomposed in contributions from three dust components of temperatures 146 K (hot dust in the ionized lobes), 44 K (warm dust in the molecular gas close to the ionization front of the lobes) and $\lesssim$20 K (cold dust in the dust bar and in the extended molecular cloud respectively)

9. Polarization by Scattering

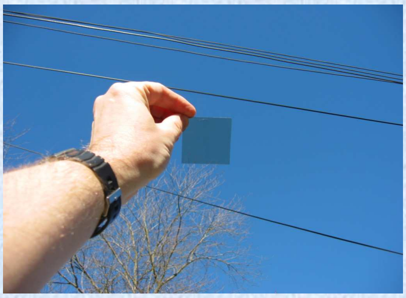
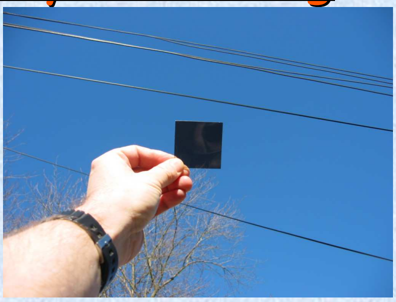

9.1. Preliminaries

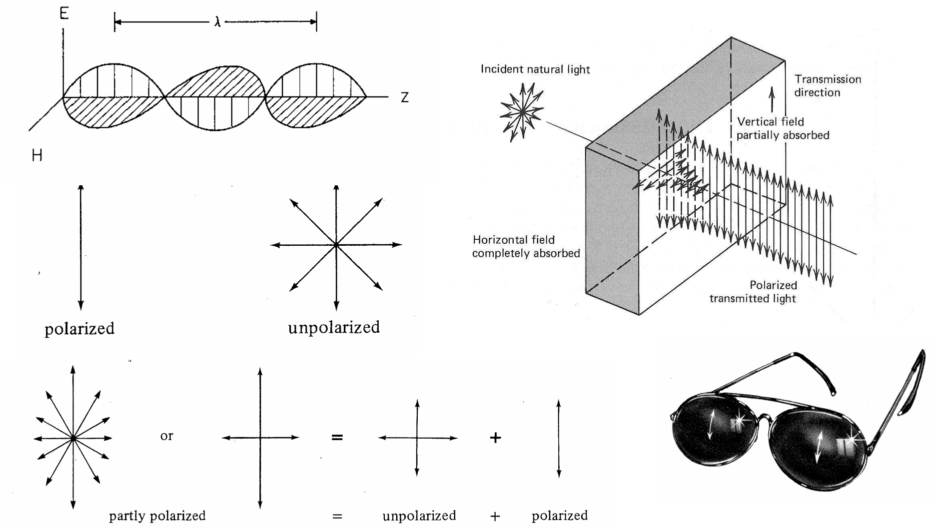

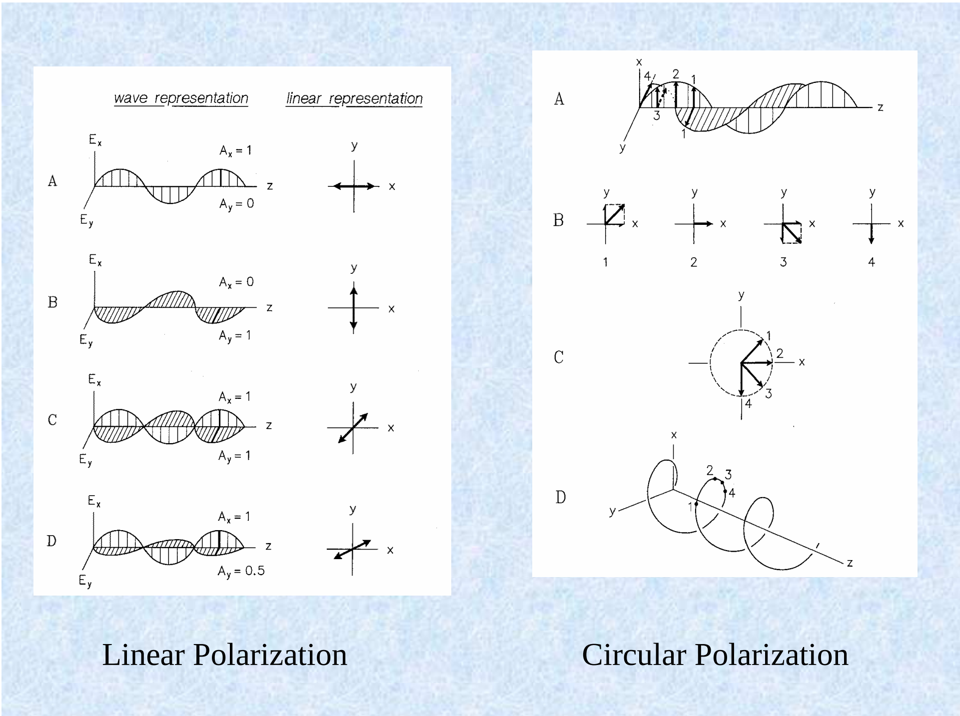

Polarization by Reflection

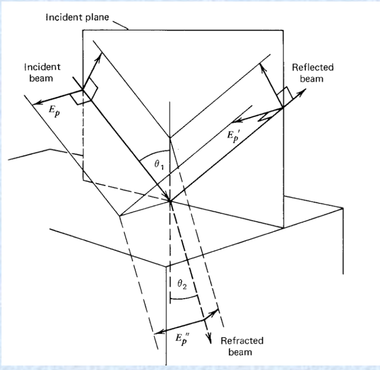

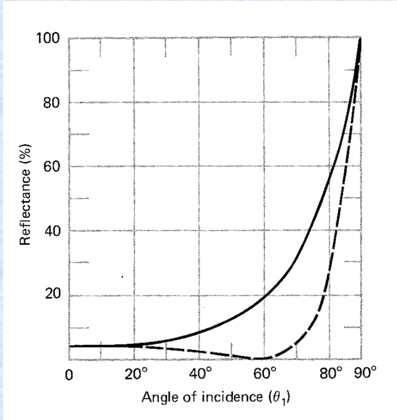

9.2. Polarization by Extinction

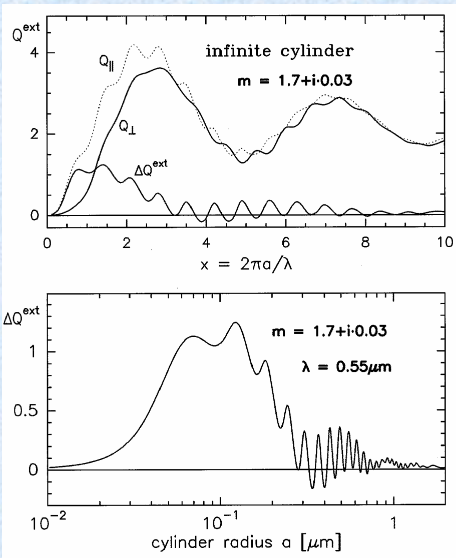

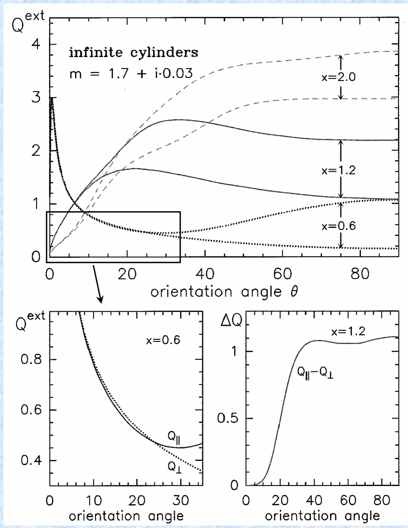

(here tip toward/away from source - 90 deg is normal incidence)

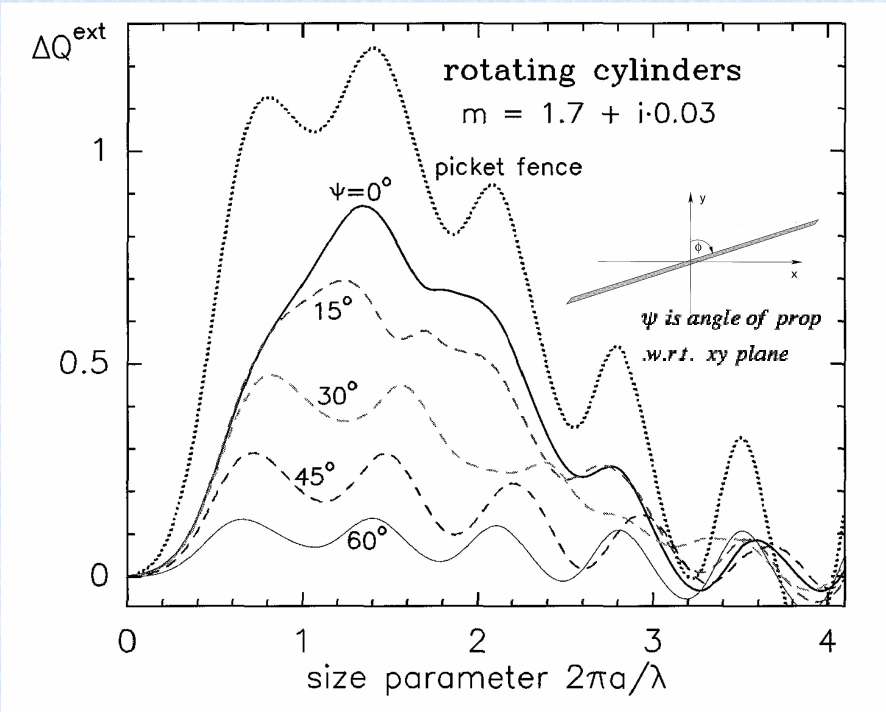

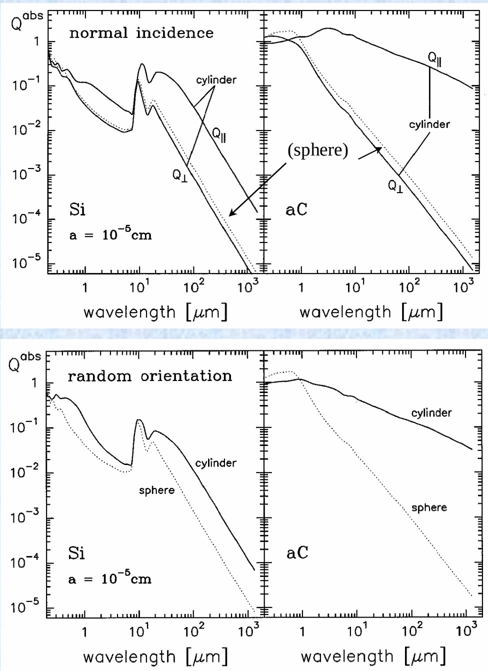

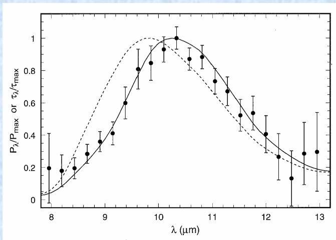

Polarization profile (solid line) and extinction profile (dotted line) in the silicate band

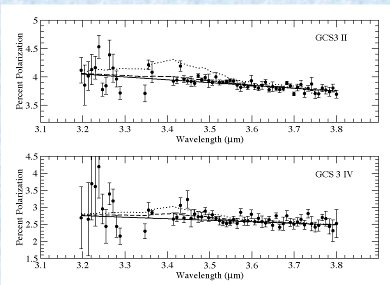

But 3.4 μm organic band is not polarized - can't be coating silicates?

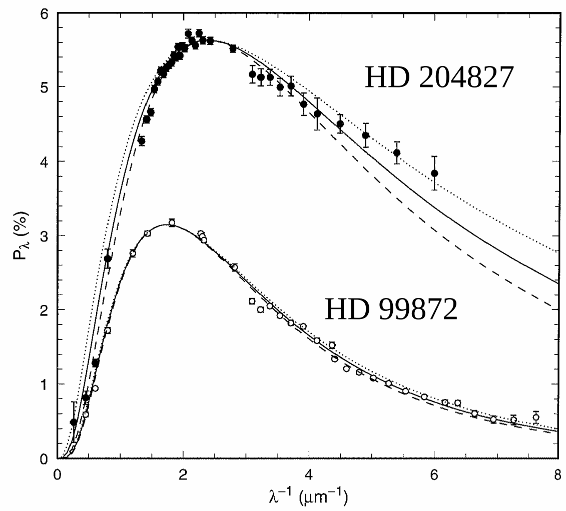

$$P_\lambda = P_{\max} \exp\left\{-K \ln^2\left(\frac{\lambda_{\max}}{\lambda}\right)\right\}$$

$$K = 1.15 \quad \text{"}\textit{Serkowski Law}\text{"}$$

$$K = c_1\lambda_{\max} + c_2 \quad \text{"}\textit{Wilking Law}\text{"}$$

Note: model fits with “astronomical silicates” seem to work better using oblate rather than prolate spheroids

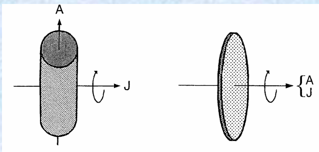

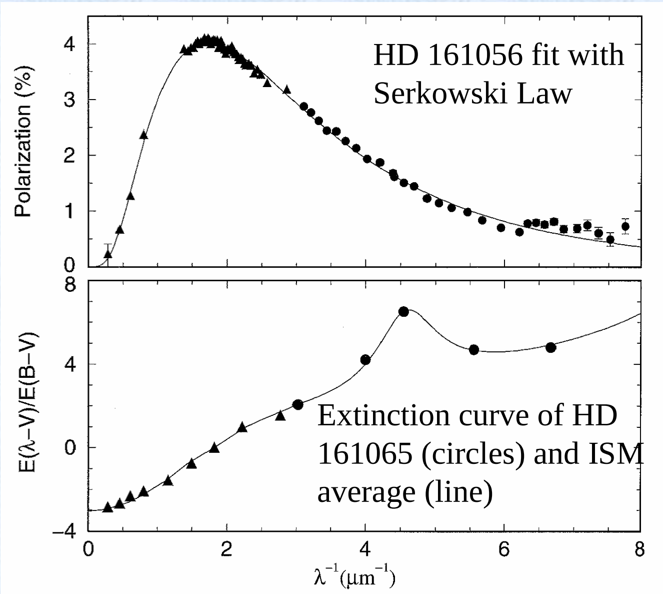

UV bump does not show up in polarization curve, so its carrier is not aligned

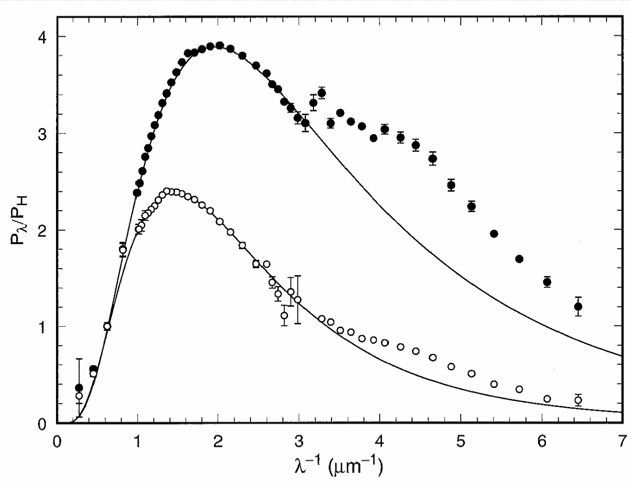

P_λ/P_H
λ^{-1} (μm^{-1})

Or is it????

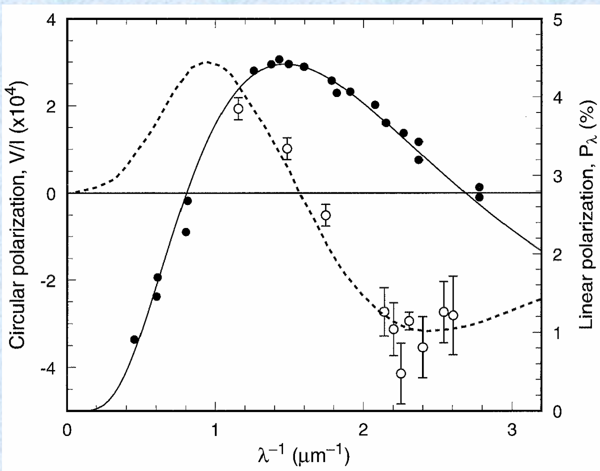

Circular polarization, V/I (x10[4])
Linear polarization, P_λ (%)
λ^{-1} (μm^{-1})

9.3. Alignment Mechanisms

•Magnetic Needles? - NO. Inconsistent with polarization maps

•Paramagnetic Relaxation (Davis-Greenstein) - Induced B-field in kT-spinning grain lags alignment - dissipative torque aligns grain. Not efficient enough?

•Superparamagnetic - like DG except uses ferromagnetic inclusions

•Suprathermal Spin (Purcell) - rocket effect via H_2 formation can achieve rotational energies greater than kT

•Radiative Torques - anisotropic radiation field - overwhelmed by collisions

•Streaming Flows (Gold) - requires unlikely organized gas flow perpendicular to galactic disk

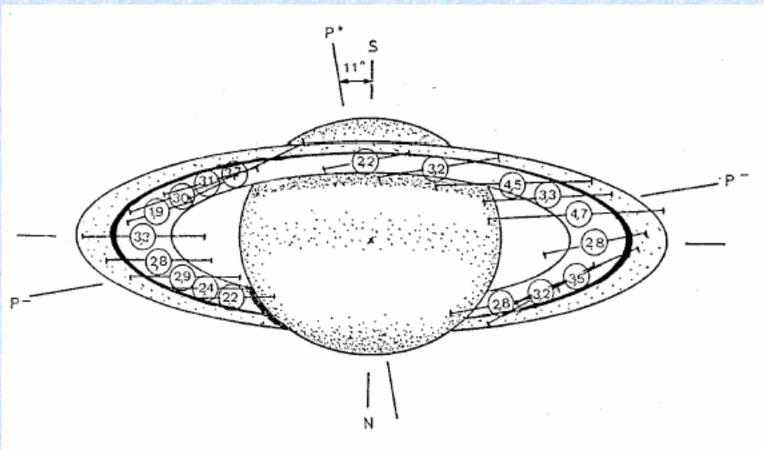

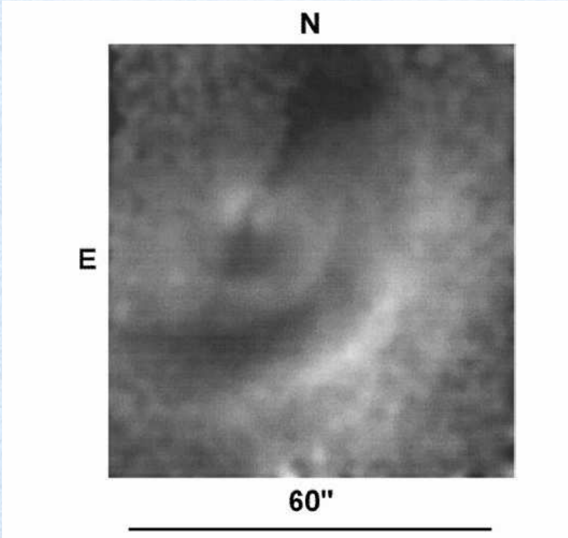

FIG. 4. Percentage polarization image of Hale–Bopp at 2.2 μm for April 1997 (c and d in Fig. 3). The dark areas correspond to 7% polarization, the bright areas to 11%. The dark streak running SE to NE is an artifact of the data analysis process. This figure has the same scale and orientation on the sky as Fig. 2.

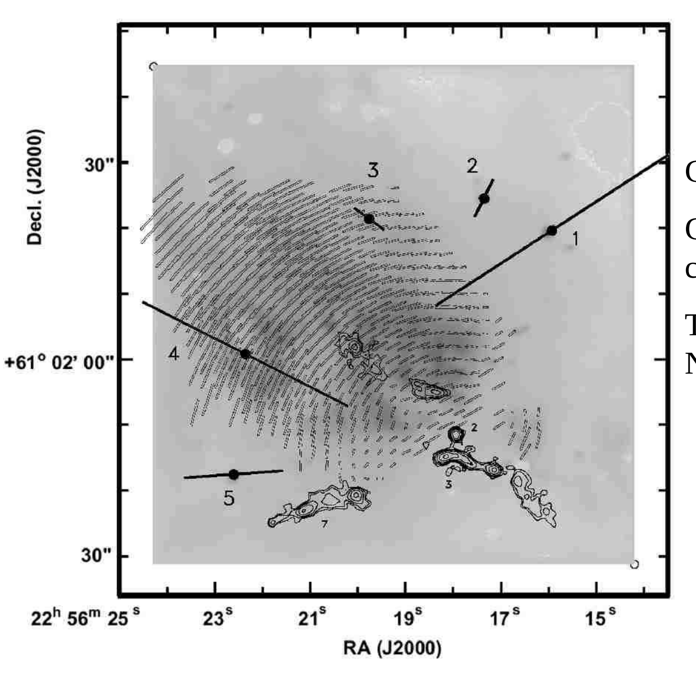

Cep A

Grayscale - radio continuum

Thin rectangles - NIR pol

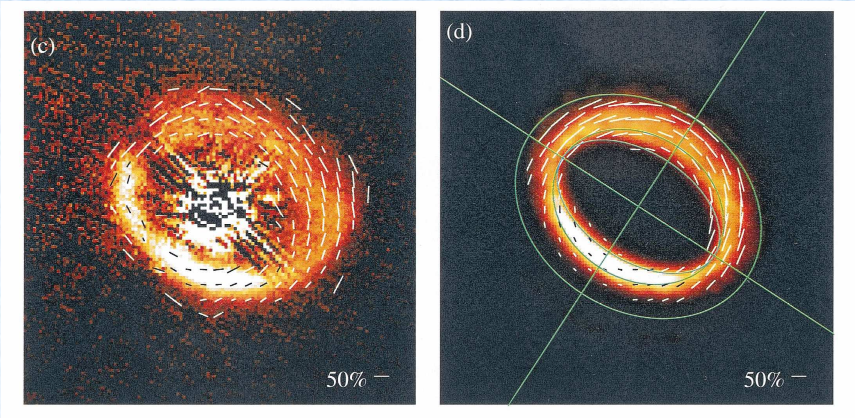

GG Tau - circumstellar ring

by way of introduction, let’s look at just intensity..

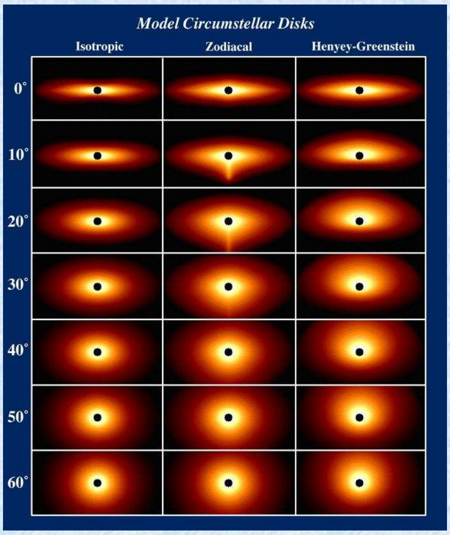

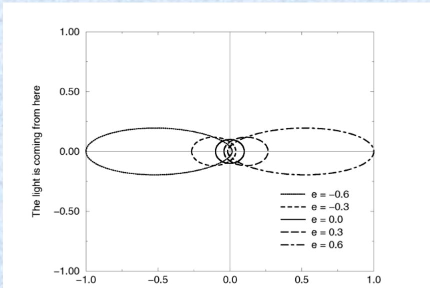

Henyey-Greenstein
Scattering Phase Function

(swiped from Dave Jewitt’s web page: http://www.ifa.hawaii.edu/~jewitt/beta.html
Their H-G model used g=-0.5, i.e. backscattering)